

See discussions, stats, and author profiles for this publication at: <https://www.researchgate.net/publication/263957924>

# Structure of Chlorine K-Edge XANES Spectra During the Breakdown of Passive Oxide Films on Aluminum

ARTICLE in THE JOURNAL OF PHYSICAL CHEMISTRY C · DECEMBER 2011

Impact Factor: 4.77 · DOI: 10.1021/jp2056305

---

CITATIONS

5

---

READS

29

## 3 AUTHORS, INCLUDING:



Donald F. Roeper

EXCET, Inc.

20 PUBLICATIONS 67 CITATIONS

SEE PROFILE

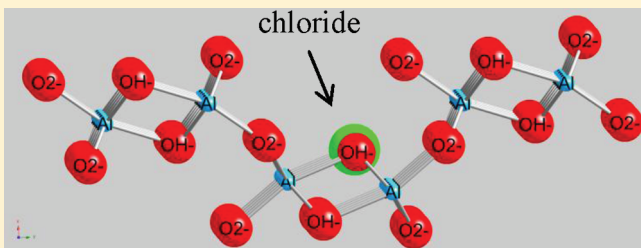
# Structure of Chlorine K-Edge XANES Spectra During the Breakdown of Passive Oxide Films on Aluminum

William E. O'Grady,<sup>\*,†</sup> Donald F. Roeper,<sup>‡</sup> and Paul M. Natishan<sup>†</sup>

<sup>†</sup>Naval Research Laboratory, Chemistry Division, Code 6134, Washington, D.C. 20375, United States

<sup>‡</sup>EXCET, Incorporated, Springfield, Virginia 22151, United States

**ABSTRACT:** We generated molecular simulations of  $\text{Cl}^-$  interacting at different sites in aluminum oxide models and carried out FEFF8 calculations to obtain the local  $l$ -projected density of states (LDOS) spectra. These are compared to our earlier experimental X-ray absorption near-edge structure (XANES) data in order to study the interactions of chloride ions with the passive oxide film on aluminum as a function of electrochemical potential at the Cl K edge. This led to a number of new insights in the mechanism of the breakdown of the passive film in chloride solutions. Importantly, we show the chloride first attacks the hydroxyl components of the aluminum oxide, penetrates the oxide film, and finally attacks the metal surface.



chloride

mechanism of the breakdown of the passive film in chloride solutions.

## ■ EXPERIMENTAL METHODS

**Electrochemical and XANES Experiments.** In this section a short review of the original experiments is presented.<sup>10,11,14</sup> Polycrystalline aluminum foils (99.999% purity) of 0.13 mm thickness were polished and then cleaned and air dried. The individual samples had an area of  $\sim 2.5 \text{ cm}^2$ , which was exposed to deaerated, room-temperature 0.1 M NaCl solution that was prepared with reagent-grade NaCl in 18  $\text{M}\Omega \cdot \text{cm}$  water. For the electrochemical experiments, a three-electrode electrochemical cell with a platinum mesh counter electrode and a saturated calomel reference electrode (SCE) were used. Individual aluminum samples were polarized at  $-850$ ,  $-800$ ,  $-750$ , and  $-700$  mV vs SCE for 1 h following a 12 h anodic polarization at their open-circuit potentials. The samples were then removed from solution, rinsed thoroughly with 18  $\text{M}\Omega \cdot \text{cm}$  water, and air dried prior to examination by XAS.<sup>10,11,14</sup>

X-ray absorption data were measured at the chlorine K edge (2822 eV) on beamline X19-A at the National Synchrotron Light Source (NSLS) at Brookhaven National Laboratory (BNL). Samples were run in a helium atmosphere, and NaCl was used as the calibration reference for the chloride edge. Electron yield and fluorescence spectra were recorded simultaneously with a combination Lytle X-ray detector. Electron yield data were used to compare to the theoretical simulations because of its much greater signal-to-noise ratio and its enhanced surface sensitivity.

**Received:** June 15, 2011

**Revised:** October 26, 2011

**Published:** November 03, 2011

## ■ INTRODUCTION

Commercially important metals and alloys such as aluminum, titanium, and stainless steels have corrosion resistance in a wide variety of environments due to the protective oxide film that forms on the surface. These oxide films can reduce or even prevent further oxidation of the underlying reactive metal. Aggressive anions such as chloride, however, can cause breakdown of the passivating oxides leading to localized corrosion in the form of crevice corrosion in occluded sites or pitting corrosion on open surfaces. There continue to be extensive discussions about the mechanisms of these reactions. Aluminum corrosion in aqueous solutions of sodium chloride has been studied extensively,<sup>1–14</sup> and the literature has recently been critically reviewed.<sup>15</sup> The prevailing mechanism describes the first step of pitting corrosion to be adsorption of chloride ions onto the passive oxide on the surface of the aluminum.<sup>1,2,7,9</sup> Once adsorbed, the chloride ion migrates through the oxide film.<sup>1–4,6,7,9–14</sup> Although the data show adsorption and incorporation in the oxide, the exact nature of the chloride interactions with the oxide film and the reaction sites have not been determined.

Using X-ray absorption spectroscopy (XAS) at the Cl K edge, interactions of chloride ions with the passive film on aluminum as a function of electrochemical potential have been probed. It was established that  $\text{Cl}^-$  interacts and is adsorbed on the surface of passivated Al metal, and then with increasing anodic potentials, the  $\text{Cl}^-$  moves into and penetrates the oxide film and migrates to the metal surface.<sup>10,11,14</sup> Using the theoretical code FEFF8, it is possible to simulate XAS spectra as well as carry out calculations of the local  $l$ -projected density of states (LDOS). We generated molecular models of  $\text{Cl}^-$  interacting at different sites in aluminum oxide models and carried out FEFF simulations to obtain LDOS spectra which are compared to our earlier experimental XANES data. This has led to a number of new insights into the

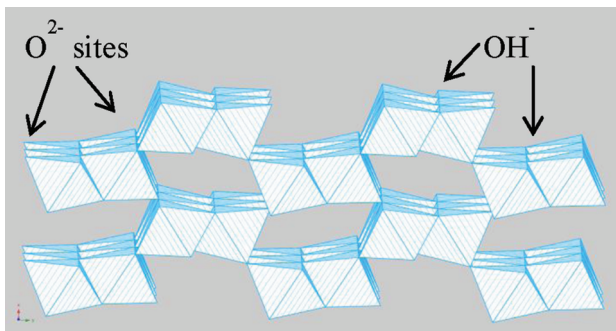


**Figure 1.** Diaspore is constructed of layers of interconnected octahedra with two oxygen sites. OH<sup>-</sup> sites have hydrogen bound to the oxygen; O<sup>2-</sup> sites are in the -2 oxidation state without hydrogen and bridge the octahedrons.

XAS data were analyzed using the standard XDAP data analysis package.<sup>16–18</sup> Additional experimental details can be found in earlier papers.<sup>10,11,14</sup>

**Theoretical Approach.** The passive oxide film that forms on the surface of aluminum and provides protection from further corrosion is not well defined and is a mix of oxide and oxyhydroxide materials which are formed from aluminum corrosion materials. However, in order to carry out theoretical calculations to determine what the electronic structure of Cl<sup>-</sup> interacting with a passivated Al surface might look like, we had to choose one of the oxides of Al as a model. The oxide initially chosen was the aluminum oxyhydroxide, diaspore,  $\alpha\text{-AlO(OH)}$ . It is well known that the film on passive Al does not have a well-defined long-range structure as using this aluminum oxyhydroxide might suggest. However, it does provide the required atomic coordinates from which to construct the theoretical models.<sup>19</sup> Initially it was chosen because it was the only oxyhydroxide for which a complete set of crystallographic atomic coordinates for the unit cell were readily available in the literature. This model suggests that the film is probably constituted of a series of building blocks formed from Al-based octahedra where the Al ions are coordinated by O<sup>2-</sup> ions, OH<sup>-</sup> ions, and H<sub>2</sub>O molecules sharing edges in small stable groups reminiscent of portions of the diaspore structure. Other aluminum oxyhydroxides such as boehmite,  $\gamma\text{-AlO(OH)}$ , have been suggested as having a structure similar to the passive film on aluminum metal, but calculations using boehmite and gibbsite,  $\gamma\text{-Al(OH)}_3$ , as models resulted in theoretical spectra that bear little resemblance to the experimental data.

Theoretical calculations were carried out using FEFF 8.0, an ab initio, self-consistent, real-space multiple scattering code for calculating XANES, X-ray absorption fine structure (XAFS), and LDOS for clusters of atoms.<sup>20</sup> This code was used to generate the XANES and LDOS for the Cl K edge for different oxide models to simulate chloride ions that penetrated into various oxygen positions of the passive aluminum oxide films. With the release of newer versions of the FEFF code it has become possible to carry out reliable calculations of XANES and the LDOS.<sup>21</sup> The LDOS provides a direct interpretation of the experimental XANES spectra and an interpretation of the electronic structures that can give rise to the structural details observed in the experimental data.<sup>21–25</sup> With calculations based upon models of chloride interacting with different sites in the aluminum oxide structure in hand, interpretation of the XANES spectral structure becomes possible. Molecular cluster sizes of approximately 87 atoms were used to carry out calculations on

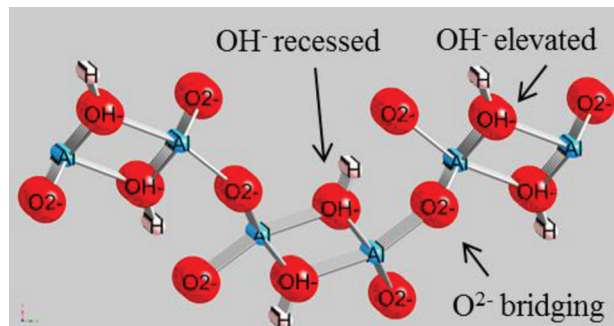


**Figure 2.** Ball and stick model of diaspore showing O positions as red balls, Al as blue balls, and H as pink balls. OH<sup>-</sup> elevated and recessed surface sites and O<sup>2-</sup> bridging sites are also illustrated.

the oxide models. The cluster was chosen such that Cl was on the flat surface of a hemisphere in order to have a symmetrical cluster while simulating the chloride to be on the surface of the oxide film. The default Hedin–Lundqvist self-energy was used for the calculations. Simulations were conducted both with the hydrogen atoms included in the model and also without using them. We found that the effect of including the hydrogen was to dampen and broaden the LDOS peaks, but the hydrogen did not add or remove any peaks. It was decided to leave the hydrogen out of the calculations so that we could use an oxide cluster of a larger size. These calculated spectra are compared directly to our previously published experimental XANES spectra of Cl interacting with the passive film on the aluminum surface as a function of the electrochemical potential.

## RESULTS AND DISCUSSION

The crystal structure of the aluminum oxyhydroxide mineral diaspore,  $\alpha\text{-AlO(OH)}$ , is illustrated in Figure 1. Diaspore is constructed of layers of interconnected octahedra with two different types of oxygen sites: sites occupied by OH<sup>-</sup> hydroxyl species and sites occupied by O<sup>2-</sup> oxygen in the bridging sites connecting the octahedra. These sites are delineated in the ball and stick model of diaspore in Figure 2, and the distinction between the elevated OH<sup>-</sup> position and the recessed OH<sup>-</sup> position is illustrated. XANES spectra observed at the selected electrochemical potentials are displayed in Figure 3, and it is seen that the Cl-edge structure undergoes significant changes as the samples are polarized sequentially to higher voltages.

In order to simulate the chloride attack and breakdown of the passive oxide film, models of the diaspore were constructed by replacing an oxygen entity from either an OH<sup>-</sup> or an O<sup>2-</sup> position with a chloride ion. There are four basic positions of oxygen on the oxide surface that could potentially be attacked by a chloride ion. The positions for the two kinds of OH<sup>-</sup> surface sites are shown in Figure 2, where the elevated site is in the highest position while the recessed surface is in the next lower octahedron but would still be directly exposed to the sodium chloride solution. The two O<sup>2-</sup> positions are the normal bridging positions, also shown in Figure 2, and the terminal position at the end of an octahedron that is not connected to another octahedron. On the basis of the spectra of the calculated LDOS for these four possible oxygen positions the OH<sup>-</sup> in the recessed surface site is the most likely initial point of attack by the chloride ion. The position of this chloride is illustrated in Figure 4a. The theoretical LDOS for the chloride ion is compared with the

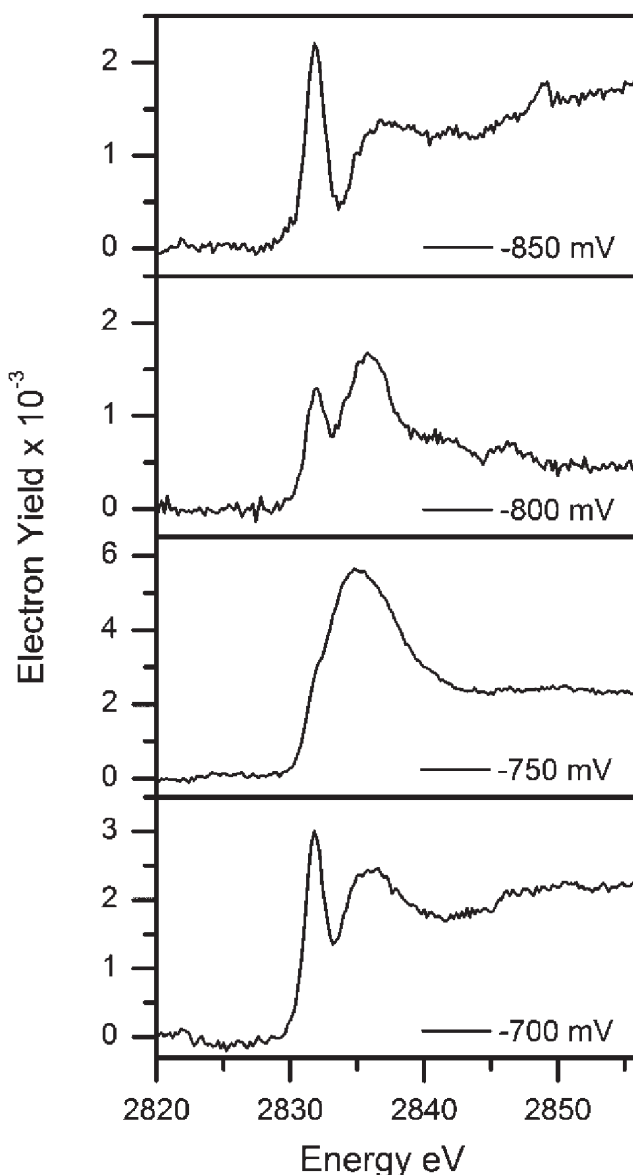


**Figure 3.** XANES spectra of aluminum foils that were anodically polarized in deaerated 0.1 M NaCl solution. Data were collected with an electron yield detector.

normalized electron yield spectrum obtained from the sample after polarization at  $-850$  mV vs SCE and is shown in Figure 4b. The first peak in the simulation lines up well with the main absorption peak, and the second peak is in the appropriate position. This position yields the best fit of the calculated spectrum with the actual data. The spectrum for a chloride in the elevated surface site has a much broader first peak that overlaps the second peak such that the second peak is only a shoulder. The model is shown in Figure 5a, and the comparison to the normalized experimental data is shown in Figure 5b. The chloride in an  $\text{O}^{2-}$  terminating site model is shown in Figure 6a, and the comparison to the normalized experimental data is shown in Figure 6b. The spectrum from a chloride in an  $\text{O}^{2-}$  terminating site is similar to the spectrum from the  $\text{OH}^-$  elevated surface site, but the first peak is even broader. The spectrum from a chloride in an  $\text{O}^{2-}$  bridging site gives a much sharper

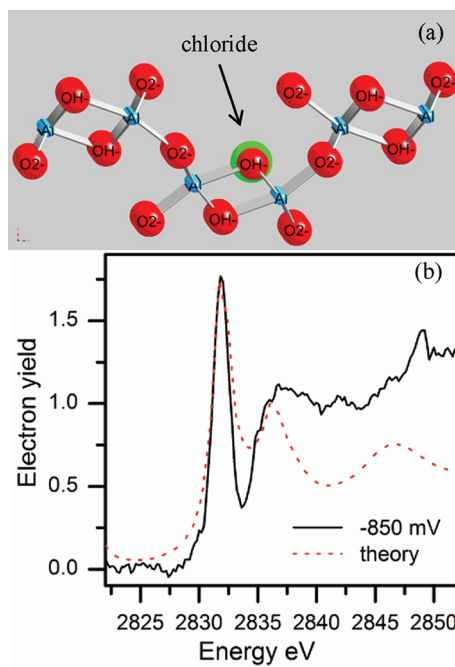


**Figure 4.** (a) Chloride ion (large green ball) is substituted for oxygen in an  $\text{OH}^-$  recessed site in the diaspore molecule. (b) Comparison of the normalized electron yield data obtained after holding the sample at  $-850$  mV, and theoretical LDOS from the chloride in the above position shows the best fit of the data.

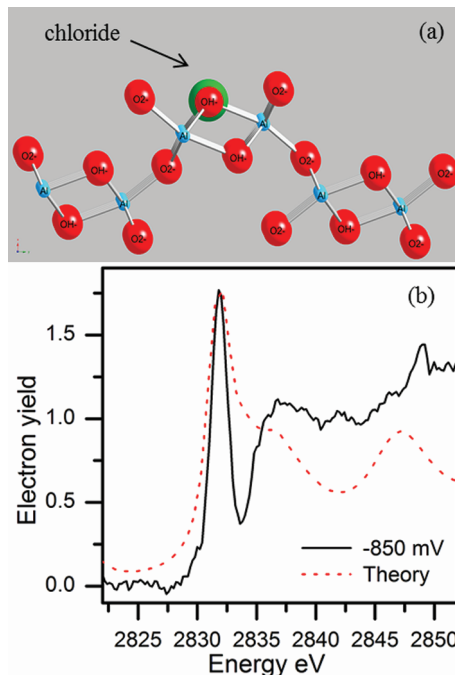


**Figure 5.** (a) Chloride ion (large green ball) is substituted for oxygen in an  $\text{OH}^-$  elevated site in the diaspore molecule. (b) Comparison of the normalized electron yield data obtained after holding the sample at  $-850$  mV, and theoretical LDOS from the chloride in an elevated surface site.

first peak that matches the experimental spectrum well, but there is a complete absence of the second peak. The chloride in this position is illustrated in the model in Figure 7a, and the

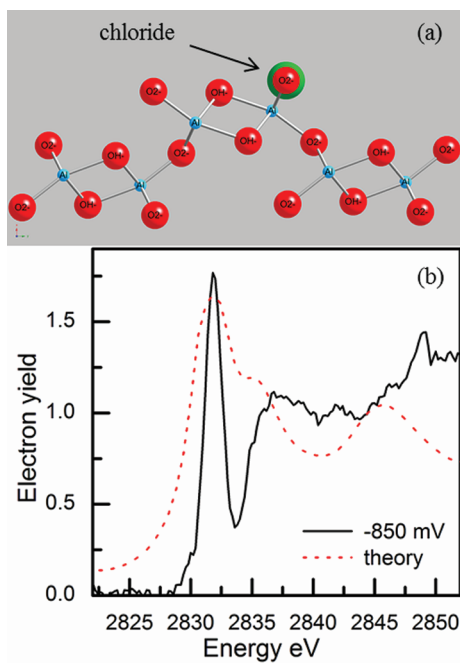


**Figure 6.** (a) Chloride ion is substituted for oxygen in an  $O^{2-}$  terminating site in the diaspore molecule. (b) Comparison of the normalized electron yield data obtained after holding the sample at  $-850$  mV, and theoretical LDOS from the chloride in an  $O^{2-}$  terminating site.

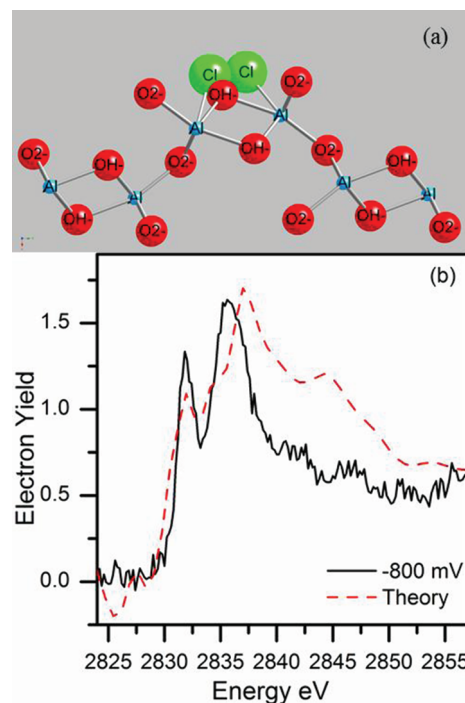


**Figure 8.** (a) Model illustrates two chlorides substituted in the diaspore molecule for one elevated  $OH^-$  site. (b) Comparison of the normalized electron yield spectrum obtained after holding the sample at  $-800$  mV, and theoretical LDOS from two chloride ions in a single  $OH^-$  site.

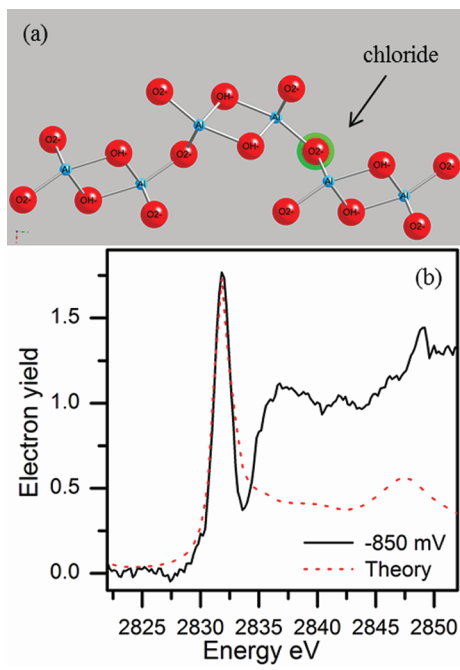


**Figure 7.** (a) Chloride ion is substituted for an oxygen in an  $O^{2-}$  bridging site in the diaspore molecule. (b) Comparison of the normalized electron yield data obtained after holding the sample at  $-850$  mV, and theoretical LDOS from the chloride in an  $O^{2-}$  bridging site.

spectrum is compared to the normalized experimental data in Figure 7b.

When the polarization potential is raised by 50 mV to  $-800$  mV a different behavior begins taking place. The first peak is

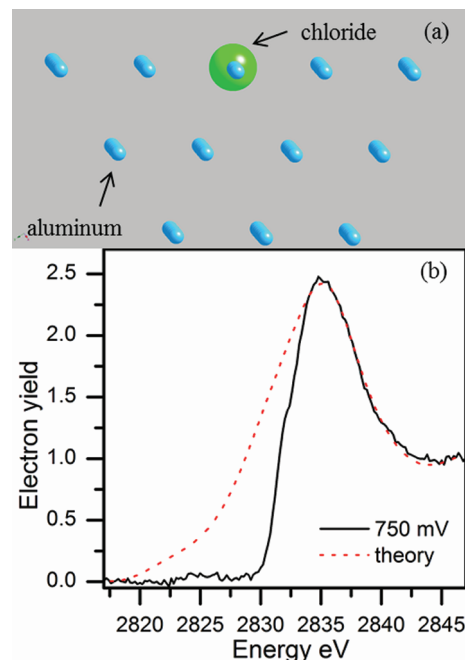


**Figure 9.** (a) Model depicts a chloride ion in the site of an aluminum atom in the (111) surface plane. (b) Comparison of the normalized electron yield data obtained after holding the sample at  $-750$  mV, and theoretical LDOS from the model shown in part a.

significantly reduced in magnitude and is now smaller than the second peak, which has remained largely the same. From a comparison of the four simulations determined for the  $-850$  mV

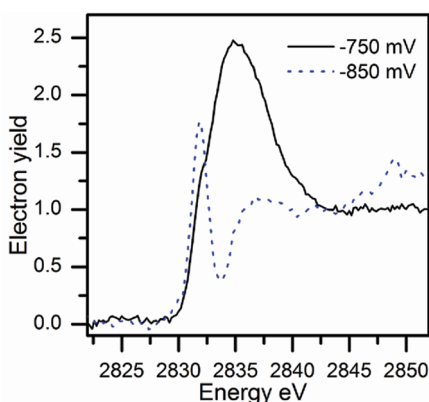


**Figure 10.** Comparison of the normalized electron yield data from  $-750$  and  $-850$  mV, demonstrating the origin of the shoulder in the  $-750$  mV data.

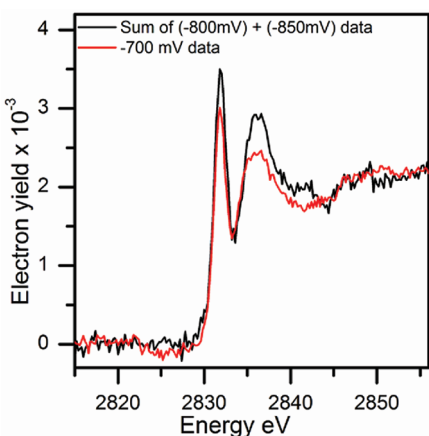


**Figure 11.** XANES data collected at  $-800$  and  $-850$  mV are summed together and compared to the XANES data collected at  $-700$  mV, demonstrating that chloride is present in multiple locations at that potential.

data for a chloride replacing an oxygen with the data for  $-800$  mV it is clear that none of the previously postulated chloride positions yield a spectrum that is comparable to the  $-800$  mV data. Figure 8a shows an illustration of the model created to simulate the data at  $-800$  mV. In Figure 8b the normalized experimental spectrum at  $-800$  mV is compared to a theoretical spectrum calculated for a model with two chloride ions placed in close proximity to one another in the position of a vacant  $\text{OH}^-$  site in an elevated surface site. The chlorides were attached to two different aluminum atoms with bond distances of  $\sim 2.0 \text{ \AA}$ , which is comparable to the shortest  $\text{Al}-\text{Cl}$  bond distance in  $\text{Al}_2\text{Cl}_6$  at  $2.06 \text{ \AA}$ .<sup>26</sup> The chloride ions are also separated from one another by  $\sim 2.0 \text{ \AA}$ . The pattern of the two peaks with the second peak higher than the first could only be generated by simulations that have at least two chloride ions that are in close proximity to each other in this aluminum oxyhydroxide system. Keeping in mind that the XAS spectrum is an average of the absorption behavior of all of the chloride ions in the system it is likely that as the pitting potential is approached all of these  $\text{OH}^-$  sites, both recessed and elevated, are going to contribute to the spectrum.

The potential was further raised to  $-750$  mV vs SCE, and the change in the experimental spectrum indicates that a completely

new chemical behavior is occurring at the interface because it is vastly different from previous spectra. The spectrum has a single broad peak that is very different from the previous spectra, and none of the previously calculated LDOS have any resemblance to it. The simulation that is found to have best matched these experimental data is that of a chloride that has reached the metal oxide interface and is interacting directly with the metal surface. This model is shown in Figure 9a. The model depicts a chloride ion replacing an aluminum atom from the aluminum surface in the (111) plane. Calculations were also made with chloride ion at various heights above the aluminum surface to simulate an absorbing chloride ion as well as slightly below to simulate a chloride ion that is strongly bonded to the metal surface. The best fit was achieved by replacing a single aluminum atom in the crystal surface structure with one chloride atom, and the results are shown in Figure 9b. There it is seen that the major peak in the XANES spectrum is reproduced very nicely. However, there is a large contribution on the low-energy side of the peak. In Figure 10 the superposition of the normalized experimental data at  $-850$  and  $-750$  mV is shown, and it is very clear that in addition to the main interaction of the Cl with the Al surface some of the interactions that are seen at the other voltages are included.

The XANES data were collected for a sample polarized at  $-700$  mV vs SCE, and a similar behavior is also observed at this voltage. None of the models constructed were able to adequately reproduce this data using a chloride in a single oxygen site. At this potential the sample is just below the pitting potential for the aluminum. Previous research has shown that the onset of stable pitting occurs at  $-690$  mV vs SCE for the polycrystalline aluminum surface in  $0.1 \text{ M NaCl}$  solutions.<sup>9,14,15</sup> Thus, at  $-700$  mV the oxide film is under aggressive attack by the chloride ions and there are likely multiple locations that have chloride ions in them as well as the effects of repassivation events caused by metastable pitting.<sup>14,27,28</sup> We were not able to develop a model which led to an acceptable fit for the XANES data collected at  $-700$  mV using a single chloride location. However, when the XANES data collected at  $-800$  and  $-850$  mV are summed together the result is very similar to the XANES data collected at  $-700$  mV, and this can be seen in Figure 11. This strongly suggests that multiple chloride sites are contributing to the spectrum at  $-700$  mV. The overall data indicates a general trend of more aggressive chloride interaction as the sample is polarized to higher voltages. As the potential is raised from  $-850$  to  $-750$  mV the chloride ions penetrate deeper into the oxide film structure and ultimately attack the aluminum metal directly. As the  $-700$  mV voltage is approached, the chloride is very aggressive and also found in multiple locations.

## CONCLUSIONS

Experimental spectra of aluminum exposed to  $\text{NaCl}$  solutions at different potentials were collected for the chlorine K edge. Calculations of the theoretical LDOS compared to the experimental data indicate that a recessed surface position of a hydroxide ion is the most likely point of initial attack when diaspore is used as the model passive film. A theoretical spectrum calculated for a chloride ion that replaces a recessed surface hydroxide ion in diaspore yields the closest match to the polarization at  $-850$  mV. When the potential is raised to  $-800$  mV it appears that the  $\text{OH}^-$  in the elevated surface sites becomes vulnerable to attack. A close match is obtained for polarization at  $-800$  mV with two chlorides in close proximity in

an elevated surface hydroxide site. Upon further polarization to  $-750$  mV the experimental data are best matched by a model where a chloride is in the surface of the aluminum lattice, but it is evident that chlorides are in additional locations as well. At the highest voltage,  $-700$  mV, the chloride has become very aggressive and is again found in several locations in the oxyhydroxide structure.

## ■ AUTHOR INFORMATION

### Corresponding Author

\*E-mail: ogrady@nrl.navy.mil.

## ■ ACKNOWLEDGMENT

We acknowledge the financial support of the Office of Naval Research and the American Society for Engineering Education. This research was carried out at the National Synchrotron Light Source at Brookhaven National Laboratory, which is supported by the U.S. Department of Energy, Division of Materials Sciences and Division of Chemical Sciences, under Contract No. DE-AC02-98CH10886.

## ■ REFERENCES

- (1) Augustynski, J. *Passivity Met., Proc. Int. Symp.*, 4th 1978, 989.
- (2) Augustynski, J.; Painot, J. *J. Electrochem. Soc.* **1976**, 123, 841.
- (3) Brown, F.; Mackintosh, W. D. *J. Electrochem. Soc.* **1973**, 120, 1096.
- (4) Chang, C.-L.; Sankaranarayanan, S. K. R. S.; Engelhard, M. H.; Shuthanandan, V.; Ramanathan, S. *J. Phys. Chem. C* **2009**, 113, 3502.
- (5) Digne, M.; Sautet, P.; Raybaud, P.; Toulhoat, H.; Artacho, E. *J. Phys. Chem. B* **2002**, 106, 5155.
- (6) Galvele, J. R. *Corros. Sci.* **1981**, 21, 551.
- (7) Kolics, A.; Besing, A. S.; Baradlai, P.; Haasch, R.; Wieckowski, A. *J. Electrochem. Soc.* **2001**, 148, B251.
- (8) McCafferty, E. *Corros. Sci.* **2003**, 45, 1421.
- (9) Natishan, P. M.; O'Grady, W. E.; Martin, F. J.; Rayne, R. J.; Kahn, H.; Heuer, A. H. *J. Electrochem. Soc.* **2011**, 158, C7.
- (10) Natishan, P. M.; O'Grady, W. E.; McCafferty, E.; Ramaker, D. E.; Pandya, K.; Russell, A. *J. Electrochem. Soc.* **1999**, 146, 1737.
- (11) Natishan, P. M.; Yu, S. Y.; O'Grady, W. E.; Ramaker, D. E. *Electrochim. Acta* **2002**, 47, 3131.
- (12) Serna, L. M.; Zavadil, K. R.; Johnson, C. M.; Wall, F. D.; Barbour, J. C. *J. Electrochem. Soc.* **2006**, 153, B289.
- (13) Wall, F. D.; Johnson, C. M.; Barbour, J. C.; Martinez, M. A. *J. Electrochem. Soc.* **2004**, 151, B77.
- (14) Yu, S. Y.; O'Grady, W. E.; Ramaker, D. E.; Natishan, P. M. *J. Electrochem. Soc.* **2000**, 147, 2952.
- (15) Natishan, P.; O'Grady, W. Chloride Ion Interactions with Oxide-Covered Aluminum and the Formation of Pits. In *Surface Chemistry of Oxide Films and Corrosion*; McCafferty, E., Ed.; Springer: New York, submitted for publication.
- (16) Koningsberger, D. C.; Mojet, B. I.; Van Dorssen, G. E.; Ramaker, D. E. *Top. Catal.* **2000**, 10, 143.
- (17) Vaarkamp, M.; Dring, I.; Oldman, R. J.; Stern, E. A.; Koningsberger, D. C. *Phys. Rev. B: Condens. Matter* **1994**, 50, 7872.
- (18) Vaarkamp, M.; Linders, J. C.; Koningsberger, D. C. *Physica B: Condens. Matter (Amsterdam)* **1995**, 208/209, 159.
- (19) Hill, R. J. *Phys. Chem. Miner.* **1979**, 5, 179.
- (20) Ankudinov, A. L.; Ravel, B.; Rehr, J. J.; Conradson, S. D. *Phys. Rev. B: Condens. Matter Mater. Phys.* **1998**, 58, 7565.
- (21) Lavrentyev, A. A.; Nikiforov, I. Y.; Dubeiko, V. A.; Gabrelian, B. V.; Rehr, J. J. *J. Synchrotron Radiat.* **2001**, 8, 288.
- (22) Ankudinov, A. L.; Rehr, J. J.; Bare, S. R. *Chem. Phys. Lett.* **2000**, 316, 495.
- (23) Rehr, J. J.; Ankudinov, A. L. *Coord. Chem. Rev.* **2005**, 249, 131.
- (24) Van Bokhoven, J. A.; Nabi, T.; Sambe, H.; Ramaker, D. E.; Koningsberger, D. C. *J. Phys.: Condens. Matter* **2001**, 13, 10247.
- (25) van der Veen, R. M.; Kas, J. J.; Milne, C. J.; Pham, V.-T.; El Nahhas, A.; Lima, F. A.; Vithanage, D. A.; Rehr, J. J.; Abela, R.; Chergui, M. *Phys. Chem. Chem. Phys.* **2010**, 12, 5551.
- (26) Palmer, K. J.; Elliott, N. *J. Am. Chem. Soc.* **1938**, 60, 1852.
- (27) Davis, B. W.; Moran, P. J.; Natishan, P. M. *Proc.-Electrochem. Soc.* **1999**, 98–17, 215.
- (28) Davis, B. W.; Moran, P. J.; Natishan, P. M. *Corros. Sci.* **2000**, 42, 2187.